

Relaxations in semicrystalline polyethyleneterephthalate using thermally stimulated currents

P. COLOMER, S. MONTSERRAT, J. BELANA*

*Departament de Màquines i Motors Tèrmics, Laboratori de Termodinàmica i Físico-química, and *Departament de Física i Enginyeria Nuclear, E.T.S. Enginyers Industrials de Terrassa, Universitat Politècnica de Catalunya, Carrer de Colom 11, E-08222-Terrassa (Barcelona), Spain*

Relaxation processes at temperatures above 20 °C in semicrystalline polyethylene-terephthalate have been studied using thermally stimulated depolarization currents (TSDC). The discharge curve shows three relaxation peaks (α_c , ρ_c and ρ^*) whose positions and intensities depend on the polarization conditions and the crystallinity. Relaxations α_c and ρ_c are heteropolar, while ρ^* may be homopolar or heteropolar according to the polarization temperature used. The effect of the crystallinity on these relaxations has been analysed by the thermal steps stimulation (TSS) method applied to an amorphous sample. Results show that α_c is fundamentally a dipolar relaxation associated with the amorphous interlamellar zone. The relaxation ρ_c is associated with the release of a free charge trapped in the amorphous regions, and ρ^* is a Maxwell–Wagner–Sillars relaxation associated with crystalline – amorphous interphases. For polarization temperatures above 150 °C, two relaxations are observed only as a consequence of overlapping ρ_c and ρ^* relaxations.

© 1998 Chapman & Hall

1. Introduction

When a non-conductive polymer is poled under suitable conditions, it may become a permanently charged material called an electret. The charging process, by application of an electrical field at a given temperature, involves dipole orientation as well as charge trapping close to the material's surface (i.e. surface charge) or distributed throughout the bulk of the material (i.e. volume charge) [1]. The charge becomes frozen by cooling the sample after thermal poling. The total induced charge and its distribution depend on the molecular structure as well as on the properties of the material.

When the electret is heated by keeping its electrodes in short circuit through an electrometer, a discharge current is obtained due to both relaxation of oriented dipoles and release of the trapped charge. The thermally stimulated depolarization currents (TSDC) technique provides vast information about transitions and relaxations in the material and their associated mechanisms [2, 3].

Polyethylene terephthalate (PET) is a polymer that can be studied either in the amorphous or the semicrystalline state at different degrees of crystallinity and perfection of the crystal. Crystallization of the sample may be carried out from the melt or from the glassy state. Measurements of small-angle X-ray diffraction, electron microscopy and viscoelastic analysis

performed in PET showing a low degree of crystallinity [4], obtained by isothermal crystallization from the glassy state, displayed the presence of two amorphous regions. One of them was attributed to an amorphous interspherulitic region and the other to an amorphous intraspherulitic region located between the crystalline lamellae.

Polarized and discharged amorphous PET films with electrodes deposited by vacuum evaporation, show two heteropolar relaxations, α and ρ , in a range of temperatures between room temperature and 100 °C. The first relaxation, α , is dipolar [5] and the ρ relaxation is due to space charge [6]. At a polarization temperature of 90 °C, the peak temperatures of these relaxations are 82 and 90 °C, respectively.

The positions and intensities of these relaxations are modified while crystallization occurs, giving rise to α_c and ρ_c relaxations in the crystalline material. By means of TSDC, Asano and Suzuki [7, 8] observed temperatures of 86 and 110 °C for α_c and ρ_c relaxations, respectively, in semicrystalline PET films with a crystalline volume fraction, χ_c , of 40% polarized for 1 h at 120 °C. A reverse current is observed at temperatures above 130 °C. Vanderschueren [9] noted a decay in intensity as well as the shift and enlarging of the dipolar peak (α) as a consequence of crystallization. Van Turnhout [10] has also studied the crystallinity effect on α and ρ relaxations, and

Belana and coworkers [11, 12] have studied the crystallinity dependence of both relaxations, applying the TSS method to an amorphous PET sample. The dependence of α on the crystallinity and the relaxation α_c have also been studied by other techniques, such as dielectric [13–15] and dynamic – mechanical [4, 16–20] analyses. According to these techniques the glass transition region clearly depends not only on the crystallinity but also on the morphological structure of the polymer.

The objective of this paper is to study the relaxations in semicrystalline PET, to analyse the influence of the different polarization parameters on them, and to assign these relaxations to concrete mechanisms.

2. Experimental procedure

Experiments were carried out on commercial PET with a number-average molecular weight, M_n , of 20000. Its determination was performed by viscosimetric measurements using *o*-chlorophenol at 25 °C as a solvent and the Marshall–Todd equation [21] as the relation between M_n and $[\eta]$

$$[\eta] = 6.56 \times 10^{-4} M_n^{0.79}$$

which is valid for the molecular weight range between 12000 and 25000.

Amorphous PET films, 2 cm in diameter and 250 μm thick, were prepared by fusion and quenching in moulds [5, 6]. Then the samples were conditioned for a few days in a vacuum chamber at 40 °C to dry them, and they were further heated to a temperature of approximately 90 °C in order to eliminate internal stresses. Density measurements after this heating process, using a density gradient column with a mixture of carbon tetrachloride and *n*-heptane at 23 °C as a solvent, yielded a degree of crystallinity lower than 5% in all cases. Aluminium electrodes were deposited on both sides of the samples, by vacuum evaporation.

Electrets were prepared, polarizing the samples by a conventional method: first, an electrical field, E_p was applied to the sample at a polarization temperature, T_p , for a time, t_p ; second, the sample was cooled down to a temperature, T_o , at a controlled rate with E_p still applied. The electrical field activated conduction mechanisms that were temperature dependent. Those mechanisms were frozen by cooling. Cooling of the samples was carried out at a rate of 2 °C min^{-1} in all cases.

Once the samples had been polarized, they were discharged by the TSDC technique. The heating rate of thermal stimulation was always 2 °C min^{-1} .

The experimental equipment included a measuring cell placed in a forced-air Heraeus oven, temperature controlled by a Setaram PID RT–3000 temperature programmer. The temperature was measured with a Mettler TM-15 digital thermometer, to an accuracy of 0.1 °C, with Pt-100 probes located very close to the sample. The temperature gradients across the sample were lower than 0.2 °C in the temperature range used. The discharge current was measured with a Keithley 616 digital electrometer whose accuracy was 5% of the reading in the range 10^{-9} – 10^{-11} A and recorded

as a function of temperature by a HP 7046 A *x*–*y* recorder.

The TSS method [11] was used to gradually increase the crystallinity of the samples. The aim of this method was to produce electrets cyclically at a fixed temperature, T_p , and then to apply to them a controlled heating up to a final temperature, T_f , whose value was increased by ΔT for each cycle. This increase was as low as possible, i.e. <1 °C in the temperature ranges where the most significant changes in crystallinity were expected. This process led to the gradual crystallization of the amorphous PET sample. The final temperatures attained, T_f , were between 90 and 140 °C. The crystallinity reached was determined by density measurements using a density gradient column. Samples of different morphology were obtained by annealing the amorphous films at different temperatures.

3. Results and discussion

TSDC curves of amorphous PET films ($\chi_c < 5\%$) polarized at 90 °C show dipolar relaxation, α , at 82 °C and space charge relaxation, ρ , at 90 °C, both are heteropolar relaxations (Fig. 1, Curve 1). TSDC curves of crystalline PET ($\chi_c = 40\%$), crystallized from the glassy state by the application of the TSS method, are shown in Fig. 1 for two polarization temperatures. Three relaxations can be observed in the thermogram: α_c , ρ_c and ρ^* .

At $T_p = 90$ °C, α_c and ρ_c are heteropolar, and they appear at temperatures of 90 and 115 °C, respectively, whereas relaxation ρ^* is homopolar and appears approximately at 130 °C. It is also observed that for temperatures higher than 140 °C the current is heteropolar again (Fig. 1, Curve 2). In the case of $T_p = 116$ °C (Fig. 1, Curve 3), α_c , ρ_c and ρ^* are heteropolar relaxations, and they appear at 92, 120 and 142 °C, respectively. The polarization temperature, as the other polarization parameters are kept constant, influences the changing position, intensity and polarity of the ρ^* relaxation.

The α_c relaxation of crystalline PET is more wide and symmetric than the amorphous α relaxation. This may be due to a wider relaxation time distribution in the first case. The apparent activation energy, E_{app} ,

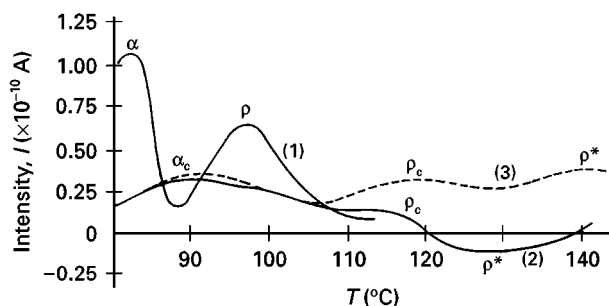


Figure 1 TSDC curves of amorphous and crystalline PET at several polarization temperatures, T_p for $E_p = 70 \text{ kV cm}^{-1}$ and $t_p = 15 \text{ min}$: (1) amorphous PET, $\chi_c < 5\%$, $T_p = 90$ °C; (2) crystalline PET, $\chi_c = 40\%$, $T_p = 90$ °C; (3) crystalline PET, $\chi_c = 40\%$, $T_p = 116$ °C.

has been determined by the initial rise of the discharge [22]. The values obtained are between 1.1 and 1.5 eV depending on the polarizing temperature. The activation energy increases when the polarizing temperature increases. This dependence of E_{app} on T_p could be a consequence of the distribution of activation energies [23]. Asano and Suzuki [7] reported apparent α_c activation energy values in the range between 0.7 and 2.0 eV depending upon whether the initial rise method or partial heating of semicrystalline PET ($\chi_c = 40\%$) was employed for the determination. The lower α_c activation energy value with respect to α relaxation in amorphous PET ($E_{app} = 3.0$ eV) [5] is confirmed by dielectric and dynamic – mechanical analyses [14].

In the case of ρ_c , the activation energy value obtained, using the initial rise method, was 2.0 ± 0.1 eV. For this relaxation, the activation energy was practically independent of the polarizing temperature. This fact could be a consequence of a process with a single activation energy. Vandershueren [9] reported values of 1.81 eV, using TSDC, and 1.67 eV by conductivity measurements.

The effect of polarization temperature on α_c and ρ_c , in crystalline PET with $\chi_c = 40\%$, is shown in Figs 2 and 3.

The maximum intensity of the relaxation α_c i.e. I_{α_c} , and the peak temperature, T_{α_c} , increase together with the polarization temperature and tend to a constant

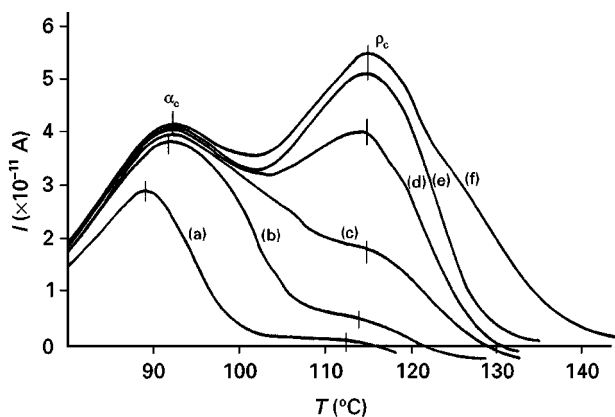


Figure 2 Polarization temperature effect on α_c and ρ_c relaxations on PET with $\chi_c = 40\%$, $E_p = 90$ kV cm⁻¹, $t_p = 30$ min and with in T_p °C: (a) 78.5, (b) 89, (c) 95, (d) 100, (e) 112, and (f) 120.

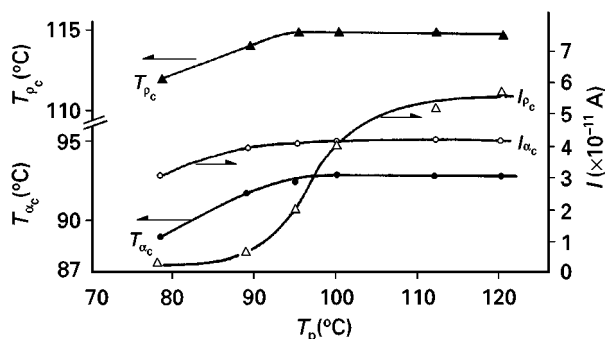


Figure 3 Intensity and temperature of α_c and ρ_c peaks versus polarization temperature, T_p , at $E_p = 90$ kV cm⁻¹ and $t_p = 30$ min.

value for $T_p > 100$ °C. The highest value of T_{α_c} is 93 °C.

On the other hand, the maximum intensity of peak ρ_c , i.e. I_{ρ_c} , and the peak temperature, T_{ρ_c} , increase with T_p . Both tend to a constant value, being the sigmoidal intensity increase. T_{ρ_c} reaches a maximum value of 115 °C for $T_p = 100$ °C, whereas I_{ρ_c} tends to reach its maximum value for $T_p > 120$ °C. In Fig. 2, it is seen that the temperature at which the current changes its sign increases with T_p . For $T_p > 112$ °C, the current does not change its sign and keeps its heteropolar character.

The polarization temperature effect on ρ^* is more complicated as this relaxation not only changes in location and intensity but also changes in polarity from homopolar to heteropolar. TSDC curves for several polarization temperatures are shown in Fig. 4. The maximum intensity, I_{ρ^*} , and the peak temperature, T_{ρ^*} , are plotted versus the polarization temperature in Fig. 5. In the case of I_{ρ^*} , only the values that correspond to the heteropolar peak have been plotted.

The maximum temperature of the ρ^* relaxation, T_{ρ^*} , varies linearly with T_p and such behaviour could indicate a barrier type mechanism associated with ρ^* . The increase of I_{ρ^*} with T_p produces a progressive overlap of this peak with ρ_c , so that, for polarization temperatures above 150 °C, ρ^* masks ρ_c completely, and only two relaxations can be distinguished: α_c , dipolar, at 93 °C, and another that takes place over a wide temperature range, composed of the overlapping ρ_c and ρ^* .

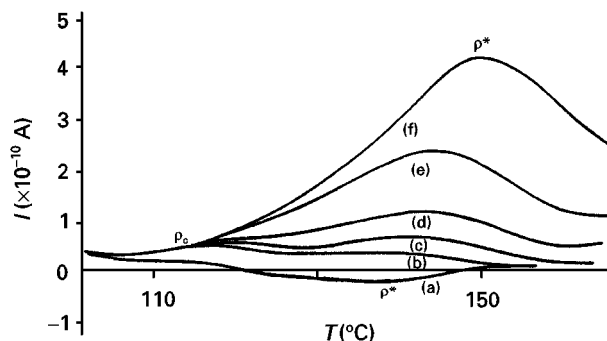


Figure 4 Polarization temperature effects on ρ^* relaxation for PET of $\chi_c = 40\%$, $E_p = 90$ kV cm⁻¹, $t_p = 30$ min, and T_p (°C): (a) 90, (b) 110, (c) 116, (d) 135, (e) 150, and (f) 170.

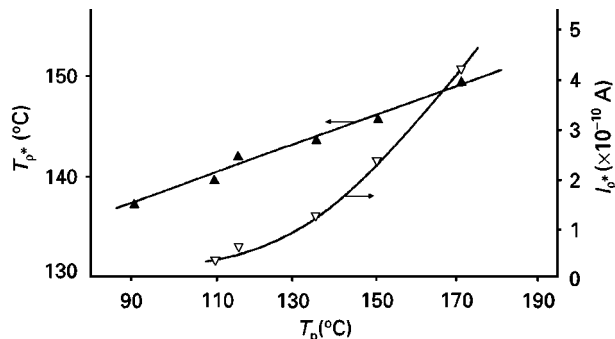


Figure 5 Intensity and temperature of ρ^* peak versus polarization temperature, T_p .

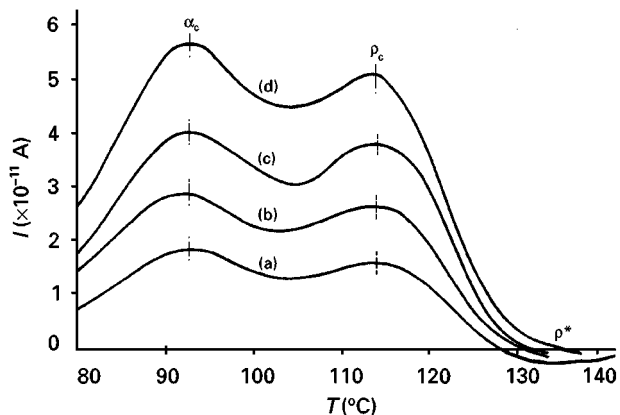


Figure 6 Effect of the applied field, E_p , on α_c and ρ_c relaxations for PET of $\chi_c = 40\%$, $T_p = 90^\circ\text{C}$, $t_p = 30$ min and E_p (kV cm^{-1}): (a) 45, (b) 68, (c) 90, and (d) 136.

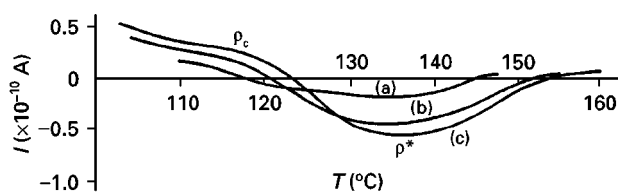


Figure 7 Effect of the applied field, E_p , on ρ^* relaxation at $T_p = 90^\circ\text{C}$, $t_p = 30$ min and E_p (kV cm^{-1}): (a) 70, (b) 135, and (c) 155.

Besides, the effects of the polarizing field on the three above relaxations, the discharge curves, for a wide range of fields have been studied and are plotted in Fig. 6 (α_c and ρ_c relaxations) and Fig. 7 (ρ^* relaxation). The peaks were isolated by the peak cleaning technique [2] to calculate the area under an individual peak without influences from the other relaxations. In Fig. 8, the intensity and the area under the curves are plotted versus the polarizing field. The polarization temperature used was 90°C , which activated α_c and ρ_c completely, and allowed the clear distinction of ρ^* , with homopolar sign, from ρ_c .

As expected, the location of peak α_c remains constant at 93°C as the peak temperature does not depend on the polarity field in polar mechanisms. The temperature of the ρ_c maximum shifts slightly towards lower values (it goes from 114 to 112°C as the field runs from 45 to 136 kV cm^{-1}). It is also observed that ρ^* inverts its current at higher temperatures and its maximum shifts to higher temperatures as the polarizing field increases.

The intensity and charge of α_c vary linearly with the polarizing field, which clearly indicates a polar mechanism. In relation to ρ_c , both magnitudes, intensity and charge, clearly deviate from linearity and tend to a constant value (saturation), which is indicative of a free charge type mechanism. In the case of ρ^* , the intensity has a clear non-linear behaviour and increases with the polarizing field, which is a consequence of the existence of a barrier type mechanism associated with this relaxation.

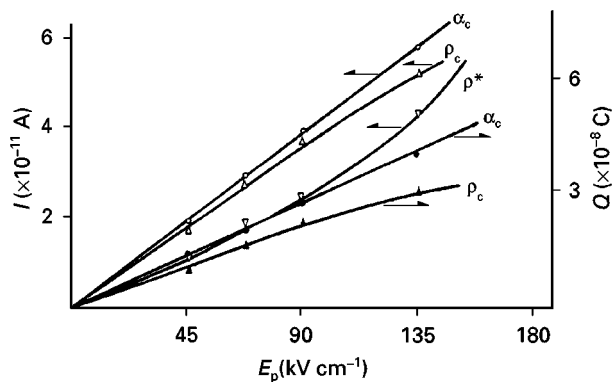


Figure 8 Charge, Q , and intensity, I , of α_c , ρ_c and ρ^* peaks versus the applied field, E_p .

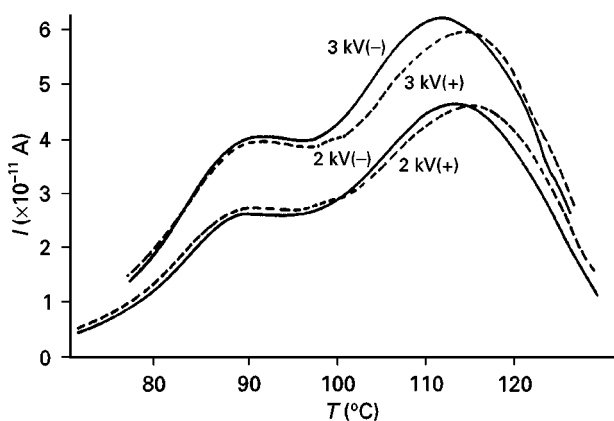


Figure 9 Electrode-polarity change effect on α_c and ρ_c relaxations at $T_p = 90^\circ\text{C}$, $t_p = 30$ min.

If the polarity of the electrode is changed, the α_c relaxation is affected either in location or in intensity, whereas ρ_c shifts to higher temperatures when the sample is biased positively. The intensity is not affected significantly, and a slight decrease in the case of high positive bias, Fig. 9, is observed.

When an amorphous PET sample is gradually crystallized by the use of the above-mentioned TSS technique, some changes are observed in α and ρ relaxations with the increase of the final temperature reached in each cycle, i.e. with the increase in crystallinity [10]. TSDC curves obtained by application of the TSS technique to an amorphous PET sample are shown in Fig. 10.

For $T_f < 105^\circ\text{C}$ ($\chi_c < 5\%$) no significant changes have been observed in α relaxation although the intensity and the maximum temperature of the ρ peak tend to increase (Fig. 10, Curves a, b). For low crystallization temperatures and for short crystallization times spherulitic growth is not possible, starting from existing nuclei, and only a nucleation process occurs. The number of nuclei increases with crystallization temperature. The restrictions to segmental mobility increase, but not sufficiently; one can see a drop of α intensity. The displacement of ρ is the result of the higher stability of the charges, influenced by the crystallinity, and the increase of the intensity is a consequence of the higher number of these charges.

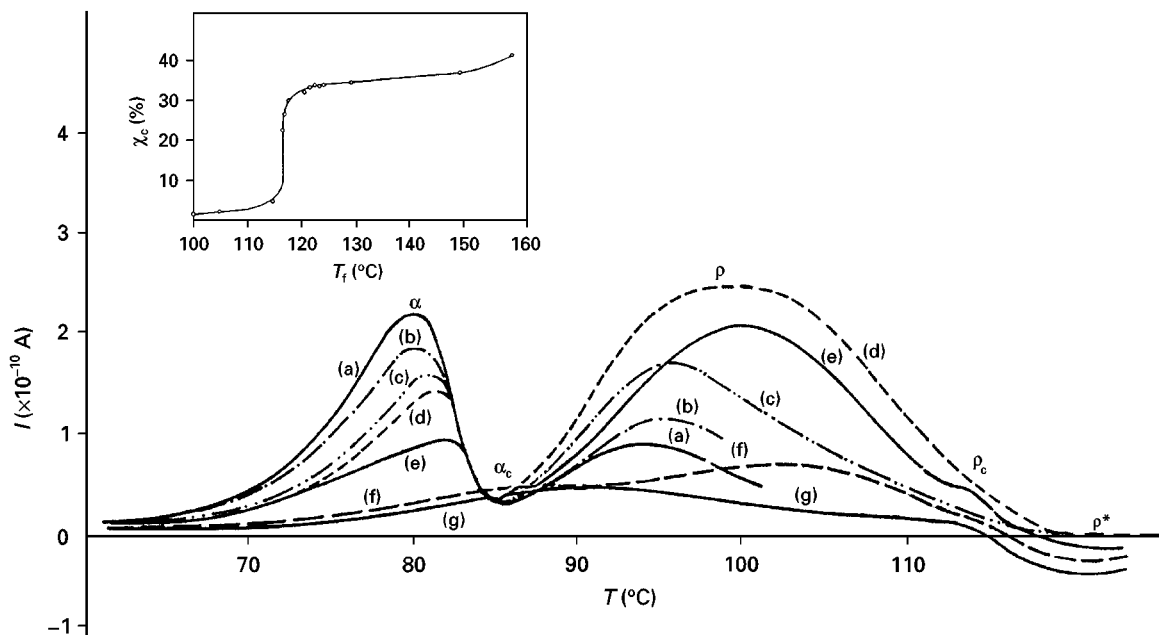


Figure 10 TSDC curves obtained by application of the TSS method to an amorphous PET sample at $T_p = 90^\circ\text{C}$, $t_p = 15$ min and $E_p = 90 \text{ kV cm}^{-1}$. The final temperature reached in the previous discharge, T_f ($^\circ\text{C}$): (a) 95, (b) 102, (c) 110, (d) 120, (e) 122, (f) 125, and (g) 130. The inset shows the crystallinity content of the PET at each final temperature.

In the T_f range between 105 and 120°C the temperature of the maximum α relaxation tends to increase progressively, while a marked fall of intensity occurs; equally, the intensity of the ρ relaxation increases sharply, going through a maximum, and the temperature of the peak also increases (Fig. 10, Curves c and d).

Initially, for T_f between 105 and 115°C (χ_c increases from 5 to 8%), nucleation is more important than spherulitic growth.

The largest number of nuclei increases the restrictions to segmental mobility and consequently decreases the intensity of the α relaxation and the peak shift maximum to higher temperatures. In the T_f range between 115 and 120°C , χ_c increases drastically as a consequence of spherulitic growth. Morphologically the sample is formed of spherulites, composed of crystalline lamellae and amorphous interlamellar region, and of an interspherulitic amorphous region [4, 17, 24, 25]. Both amorphous regions, with different restrictions to the segmental mobility, originate two dipolar relaxations, α and α_c , and two free charge relaxations, ρ and ρ_c . The α and ρ relaxations are assigned to the amorphous interspherulitic region of the amorphous material, and α_c and ρ_c to the amorphous interlamellar region of the spherulites.

For $T_f = 122^\circ\text{C}$ ($\chi_c = 32\%$) (Fig. 10, Curve e), the ρ relaxation initiates a fast decrease in intensity, while the intensity of the α relaxation falls sharply. When this decrease of intensity of the ρ relaxation is taking place, α_c and ρ_c relaxations can be observed in the spectrum together with α and ρ . The presence of α_c and ρ_c relaxations in crystalline PET of low crystallinity suggests the possibility of two glass transition temperatures [26]. Results obtained by mechanical measurements [24], TSDC [11, 25, 27, 28] and en-

thalpy relaxation [29] show the presence of a double α relaxation. Physical ageing of semicrystalline PET affect both relaxations, but the kinetics of structural relaxation are different in either case because the mobility of the chain segments in each region is different [29]. The double α relaxation disappears with an increase of crystallinity content as a consequence of the restrictions to mobility in the amorphous interspherulitic region.

Relaxation ρ^* is perceptible in the discharge when ρ reaches its maximum intensity, so that ρ^* develops while ρ is decreasing and shifting. The ρ^* relaxation appears at approximately 125°C . The decrease in ρ is a consequence of the increase in size of the spherulites and, therefore, of the increase in crystallinity. For this reason the development of ρ_c and ρ^* could be associated with the increase in crystallinity and, therefore, with the amorphous interspherulitic region and the amorphous-crystalline interphases, respectively. When the maximum degree of crystallinity is reached, $T_f > 125^\circ\text{C}$, both α and ρ disappear from the spectrum and only α_c , ρ_c and ρ^* remain visible in the spectrum (Fig. 10, Curves f, g).

4. Conclusions

In view of the effect of the studied parameters it is concluded that α_c is a relaxation of polar origin, related to the interlamellar amorphous region; the ρ_c relaxation is attributed to a free charge related to detrapping in amorphous regions, very much influenced by the crystallinity and the morphology of the material; and finally, ρ^* originates from the free charge associated with amorphous-crystalline interphases and, therefore, it is related to a Maxwell-Wagner-Sillars mechanism.

Acknowledgements

Financial support was provided by the Plan Nacional de Nuevos Materiales of the Comisión Interministerial de Ciencia y Tecnología (CICYT), Spain, Project No. PB 93-1241.

References

1. J. VAN TURNHOUT, "Electrets", Topics in Applied Physics, Vol. 33, edited by G. M. Sessler (Springer-Verlag, Berlin, 1980).
2. J. VANDERSCHUEREN and J. GASLOT, "Thermally stimulated relaxation in solids", Topics in Applied Physics, Vol. 37, edited by P. Braülich (Springer-Verlag, Berlin, 1979).
3. J. BELANA, PhD thesis, Universidad de Barcelona, Barcelona (1978).
4. G. GROENINCKX, H. BERGHMANS and G. SMETS, *J. Polym. Sci., Polym. Phys. Ed.* **14** (1976) 591.
5. J. BELANA, P. COLOMER, S. MONTSERRAT and M. PUJAL, *Anales Fisica B* **78** (1982) 8.
6. *Idem.*, *ibid.* **78** (1982) 142.
7. Y. ASANO and T. SUZUKI, *Jpn. J. Appl. Phys.* **11** (1972) 1139.
8. *Idem.*, *J. Appl. Phys.* **44** (1973) 1378.
9. J. VANDERSCHUEREN, PhD thesis, Université de Liège, Liège (1974).
10. J. VAN TURNHOUT, "Thermally stimulated discharge of polymer electrets" (Elsevier, Amsterdam, 1975).
11. J. BELANA, P. COLOMER, M. PUJAL and S. MONTSERRAT, *Polymer* **29** (1988) 1738.
12. J. BELANA and P. COLOMER, *J. Mater. Sci.* **26** (1991) 4823.
13. P. HEDVIG, "Dielectric spectroscopy of polymers" (Hilger, Bristol, 1977).
14. N. G. McCRUM, B. E. READ and G. WILLIAMS, "Anelastic and dielectric effects in polymer solids" (Wiley, New York, 1967).
15. J. C. COBURN and R. H. BOYD, *Macromolecules* **19** (1986) 2238.
16. T. MURAYAMA, "Dynamic mechanical analysis of polymer materials" (Elsevier, Amsterdam, 1978).
17. K. H. ILLERS and H. BREUER, *J. Colloid Sci.* **18** (1963) 1.
18. M. TAKAYANAGI, H. YOSHINO and S. MINAMI, *J. Polym. Sci.* **61** (1962) 173.
19. J. H. DUMBLETON and T. MURAYAMA, *Kolloid Z.Z. Polymer* **220** (1967) 41.
20. S. SAITO, *ibid.* **189** (1963) 116.
21. J. MARSHALL and A. TODD, *Trans. Faraday Soc.* **49** (1953) 67.
22. G. F. J. GARLICK and A. P. GIBSON, *Proc. Phys. Soc.* **60** (1948) 574.
23. V. HALPERN, *J. Phys. D: Appl. Phys.* **27** (1994) 2628.
24. K. H. ILLERS, *Kolloid Z.Z. Polymer* **245** (1971) 393.
25. G. VIGIER, J. TATIBOUET, A. BENATMANE and R. VASSOILLE, *Colloid Polym. Sci.* **270** (1992) 1182.
26. R. F. BOYER, *J. Polym. Sci., Polymer Symposia* **50** (1975) 189.
27. A. BERNES, D. CHATAIN and C. LACABANNE, *Thermochem. Acta* **204** (1992) 69.
28. *Idem.*, *Polymer* **33** (1992) 4682.
29. S. MONTSERRAT and P. CORTES, *J. Mater. Sci.* **30** (1995) 1790.

Received 24 June 1996
and accepted 5 December 1997